Article ID:1006-3471(2001)01-0030-07

The Applications of Confocal Raman Micro-Spectroscopy for study of practical electrode materials

YANG Y* CHU W, NAN J M, CHEN X G, LIN Z G
(State Key Lab for Phys. Chem. of Solid Surface, Xiamen Univ., Xiamen, 361005, China)

Abstract: Some recent research work about applications of confocal Raman micro-spectroscopy for study of practical electrode materials carried out in our lab has been briefly introduced. The examples include study of electrochemical Li^+-intercalation process, characterization of surface oxide film on AB_5-type electrodes and passive film and pitting corrosion of Rebar electrodes.

Key words: Li^+-intercalation electrodes, spinel $LiMn_2O_4$ electrodes, AB_5-type metal-hydride electrodes, surface oxide film, pitting corrosion, Rebar eletrodes, confocal Raman spectroscopy.

CLC Number: O 646, O 433 Document Code: A

1 Introduction

To understand relationship between structure and properties of electrode material or surface films on the electrodes is a very important subject in electrochemical field. Raman spectroscopic technique is a very useful tool to investigate the vibrational properties of electrode materials such as metal-oxide system especially at low frequency region where strong absorption of water occurs in far-infrared region. In the last few years, we have explored to use confocal Raman micro-spectroscopy for study of some important practical electrode materials or surface oxide films on the electrodes[1~5] which they are widely used as batteries' electrodes or construction materials i.e. Rebar in cement. Some useful information has been obtained for understanding of composition of the surface species formed during the electrode reactions in these electrochemical systems. In this paper, some results about our studies will be briefly reviewed mainly based on our lab's research

Received date: 18 Oct. 2000

* Corresponding author

Foundation item: Projects were supported by National Natural Science Foundation of China (No. 29925310, 29833090, 29673003)

work. The detailed results and discussed can be found in the published or the following to be published papers.

2 Experimental

Detailed description of electrode materials, chemical reagent, pretreatment conditions can be found in the literature[1~5]. Most of electrochemical measurements were performed by PARC 263/273 A potentiostat/gavalnostat (PARC, USA) or IM6 impedance spectrum analyzer (ZAHNER-elektrik, Germany). Raman experiments were carried out with a Confocal Microprobe Raman system (Labrum I from Dilor, France). The excitation light was from an air-cooled He-Ne laser (623.8 nm). According to different experiments, the laser power is different. e.g. in $Li_xMn_2O_4$ experiments, the laser power is better less than 1mW, however, in metal-hydride electrode system, the laser power can be higher at about 13 mW. The diameter of the laser spot was controlled at 1~10 μm.

3 Results and Discussion

3.1 Raman spectroscopic study of Li-deintercalation process in spinel $Li_xMn_2O_4$ materials[1~2]

In the first system, structural changes of the spinel electrode materials $LixMn_2O_4$ doping with different amount of Li^+ ions and during the electrochemical intercalation/de-intercalation cycles have been investigated. It has been shown that ex-situ confocal Raman spectroscopy can sensitively distinguish the different phases between $0 < x < 0.5$ and $0.5 < x < 1$ in spinel $LixMn_2O_4$ at peak around 620 cm^{-1}. In electrochemically modulated Raman spectroscopy (see Fig. 1), the changes of the peak around 590 cm^{-1} shows that there are two steps in Li^+ intercalation/de-intercalation reactions of $LixMn_2O_4$ (see Fig. 2). Based on the theoretical analysis[6] and literature results[7], The peaks at 620 cm^{-1} and 590 cm^{-1} are attributed to the T_{2g} and A_{1g} vibration mode of Mn *. O bond in λ-MnO_2. In addition, as decreasing of the electrode potential, i.e. as intercalation of Li^+ into λ-MnO_2 lattice, the Raman peak shifts to lower frequency, this result indicate that the intercalation of Li^+ into $Li_xMn_2O_4$ not only weakens the Mn-O bond but also causes the expansion of the crystal lattice. Thus it can be observed that the Raman shift moves to lower frequency and increase of lattice parameters which cal-

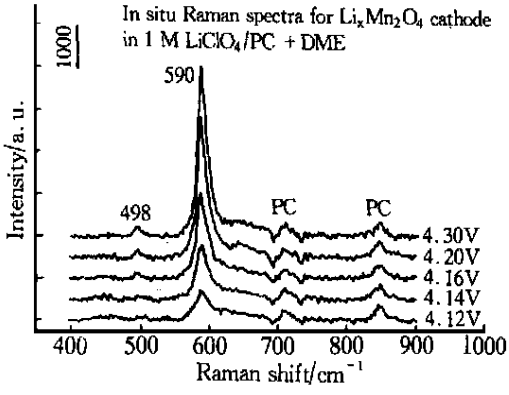

Fig. 1 In situ Raman spectra of $LixMn_2O_4$ at different potentials in 1 mol/L $LiClO_4$/PC + DME. The electrode potential and possible origin of Raman peaks for PC solvent are also labelled in the figure

culated from XRD data respectively.

3.2 Raman spectroscopic study of surface oxide film on AB_5-type metal hydride electrodes[3~4]

In the second system, the structural changes of surface oxide film on metal-hydride electrodes have been characterized by using in-situ and ex-situ Raman micro-spectroscopy. On the basis of Raman and electrochemical experimental results, it is concluded that nickel played a primary role in the composite surface oxide layer formed on the surface layer of MH electrode. On the other hand, based on in-situ and microscopic Raman results, it is also demonstrated that La, Co, Mn and other alloy components segregated and enriched progressively to alloy surface layer due to their affinity with water, and subsequently produced oxides during charge-discharge processes. Fig. 3 shows two Raman spectra of "activated" electrodes, one is the spectra of surface oxide film on crack site, another is the spectra of surface oxide film on smooth site on the electrode surface, based on the literature results[8~12] and our own results besides some of Raman peaks at 474.6 and 555.6 cm^{-1} are assigned to the formation of higher valence nickel oxides from its divalent oxide, four weaker and less well-defined Raman peaks (i.e. 430.2, 494.1, 597.8 and 635.8

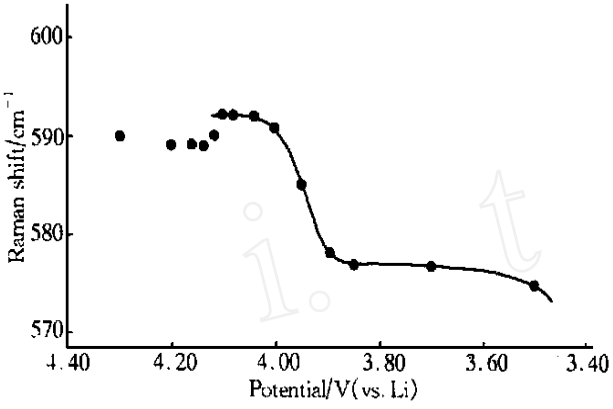

Fig. 2 Potential-dependence of the Raman peak for Mn-O bond at around 590 cm^{-1}

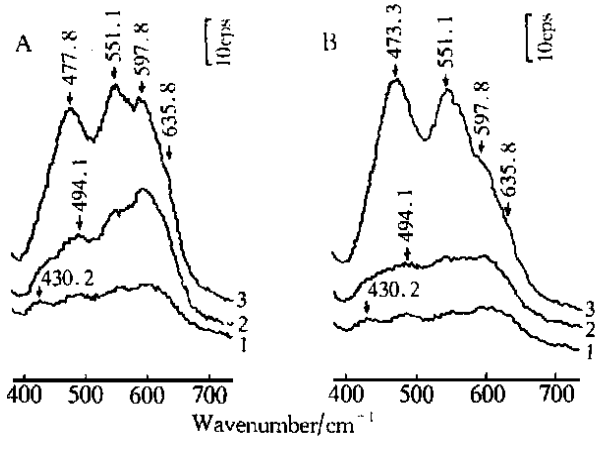

Fig. 3 In-situ Raman spectra for activated MH electrode at different sampling spots, A: sampling spot with crack, B: sampling spot without visible crack, 1): -0.2 V, 2): 0.2 V, 3): 0.35 V

cm^{-1}) are also primarily ascribed. i. e. the peaks at 430 cm^{-1} and 597.8 cm^{-1} to $Co(OH)_2$ and CoO, and the peaks at 494.1 cm^{-1} and 635.8 cm^{-1} to $Mn(OH)_2$ and MnO. It also indicates that the difference in composition between crack and smooth sites on the electrode surface.

In addition, confocal Raman microscopy has also been explored for study of powder MH electrodes. It is shown that non-uniform distribution of oxides on different alloy particles. Fig. 4 shows some Raman spectra of practical powder electrodes after 500 charge-discharge cycles. It shows that different composition of surface oxide on each alloy particles and can even look at mixture binders by using confocal Raman microscopy.

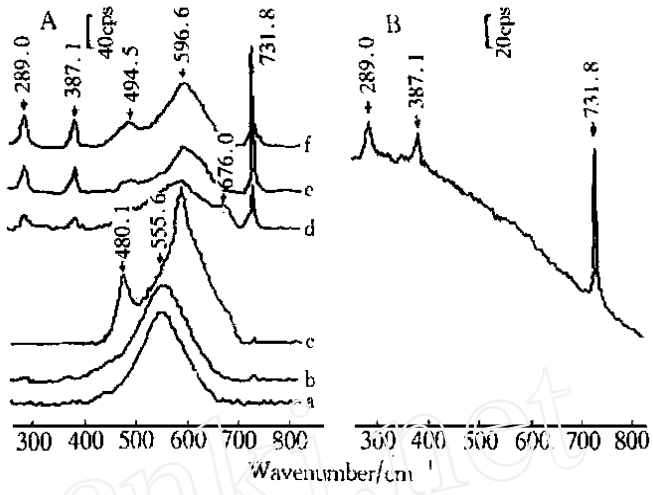

Fig. 4　A: Raman spectra for the powder MH electrode after 500 charge-discharge cycles at open-circuit potential at different sampling spots; B: Raman spectra for mixture binder

3.3　Raman spectroscopic study of passive films on carbon steel (Rebar) electrodes in simulated cement solutions[5]

In the third system, microprobe Raman spectroscopy and photoelectrochemical microscopy (PEM) were combined and applied in studying the composition and local electronic properties of the passive film on the REBAR electrode surface formed in simulated cement pore solution. Although some normal Raman spectroscopy have been used[13~15] in the study of passive films on iron electrodes in acid or alkaline solutions, however, confocal Raman microscopy have not been used in the study of passive films on Rebar electrodes before this work. Two growth-modes of passive films such as potential-scanning- and single-potential-step growth modes have been investigated and compared. Fig. 5 shows a set of Raman spectra of surface oxides which formed in two growth modes and at pristine state. It indicates that two-type of passive films with different structure and compositions are formed by these two growth modes. For example, it has been demonstrated that a amorphous film mainly containing ferrous-oxides which was formed by single-potential step polarization, however, a multi-layer structure oxide film which was formed by potential-scanning (or oxidation-reduction cycles, ORC) method. The formation and transformation of the films under different electrochemical conditions are discussed based on our results. In addition, we have also explored the advantages of the confocal Raman microscopy in the study of spa-

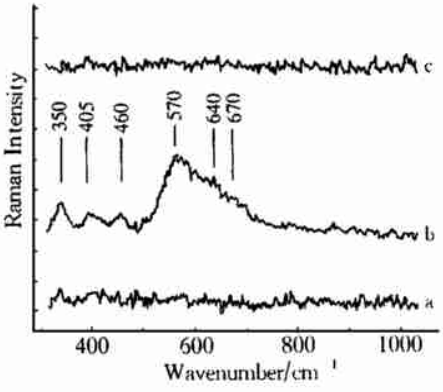

Fig. 5 Raman spectra of the electrodes obtained at different potentials. a: −1.2 V after the electrode was reduced at −1.2 V for 20 minutes; b: after oxidation-reduction cycles and measured at 0.7 V; c: when the electrode was oxidized at 0.7 V directly stepping from open circuit potential to +0.7 V for 30 min.

Fig. 6 CCD image of pitting corrosion of passive film on Rebar electrode in simulated cement pore solution (pH = 12.5) containing 10% NaCl. The black region represents corrosive pit.

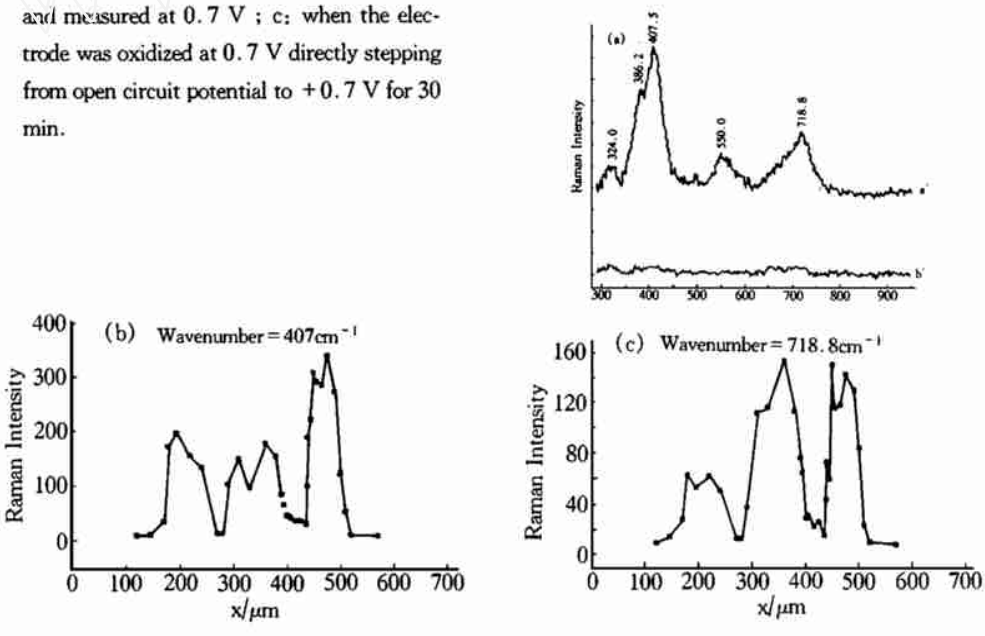

Fig. 7 a) Raman spectra of passive films on the corrosive pit(a') and smooth site on Rebar electrodes. b) Profile of "line-scan" of the spectral peak at 407 cm^{-1} along the line (1 −>2) labeled in Fig. 6. c) Profile of the peak at 718.8 cm^{-1} similar to b).

tial distribution of passive film formed during localized corrosion such as pitting corrosion processes. Fig. 6 shows a CCD image of pitting corrosion of Rebar electrode in simulated cement pore solution (pH = 12.5) containing 10 % NaCl. The black region represents corrosive pit. Fig. 7a shows

a comparison of Raman spectra of oxide film between pit site and without pit site. In addition, the profiles of "line scanning" by collecting of spectral line at 407.5 and 718.8 cm^{-1} along the point 1 to point 2 in Fig. 6 are also shown in Fig. 7b and 7c. It is clearly seen that different distribution of surface oxide species in the passive films on corrosive electrodes.

Acknowledgements:

The authors are grateful for the financial support from National Science Foundation (No. 29673003 29833090) and New Material Division of National High-Technology Research and Development committee. We would like to thank Prof. Z. Q. Tian, Dr. B. Ren, Mr. Q. J. Huang, Ms. X. Q. Li, Mr. J.L. Yao for assistance with Raman experiments. Y. Yang would also like to thank additional financial support from NSFC(No..29925310) for an excellent young scholar research award and additional support from department of education, PRC.

References:

[1] Chu W. Structure, performance and characterization of manganese nodule, $LiMn_2O_4$ and other cathode materials for lithium ion batteries[D].. Xiamen University, 1999.

[2] Chu W, Zhang Z R, Liu Z T, Yang Y, Lin Z G. In-situ and ex-situ Raman spectroscopic characterization of Li^+-intercalation processes and structural changes of spinel or modified spinel materials[C], in "Micro Power Sources" edited Zaghib K and Surampudi S, PV2000-3, The Electrochemical Society Inc, 125.

[3] Nan J M. Effects of surface ppretreatment on surface properties and performances of AB_5-type hydrogen storage alloy electrode for MH/Ni Battery[D]. Xiamen University, 1998.

[4] Nan J M, Yang Y, You J K, Li X Q, Lin Z G. In-situ and ex-situ characterization of surface oxide films on AB_5-type metal-hydride electrodes[J]. J. Alloys and Compounds, 1999, 293 - 295:747.

[5] Chen X G. The Composition, structure and in-situ spectroscopic characterization of passive films on iron-based electrodes[D]. Xiamen University, 1997: b) Chen X G, Yang Y, Lin Z G. In-situ spectroscopic and scanning probe microscopic characterization of passive films on iron-based electrodes, in proceeding of symposium on "passivity and breakdown", The Electrochemical Society Inc[C]. 1997:180～184.

[6] Ammundsen B A, Burns G R, Roziere J, et al. Lattice dynamics and vibrational spectra of lithium manganese oxide: A computer simulation and spectroscopicstudy[J]. J. Phys. Chem. B. 1999, 103:5 175.

[7] Huang W, Frech R. In-situ Raman spectroscopic studiess of electrochemical intercalation in $Li_xMn_2O_4$-based cathodes[J]. J. Power Sources, 1999:81～82.

[8] J. F. Jackovitz. Proceedings of the Symposium on the Nickel Electrode[C]. edited by R. G. Gunther, S. Gross. The Electrochem. Soc. Inc., Pennington, N J, PV82～4, 48～68.

[9] Cornilsen C, Karjala P J, Loyselle P L. Structural comparison of nickel electrodes and precursor phases[J]. J. Power Sources, 1990, 22:351 and reference therein.

[10] Melendres C A, Paden W, Tani B, Walczak W. On the structure of the higher oxide forms of nickel[J]. J. Electrochem. Soc., 1987, 134:762.

[11] Melendres C A, Pankuch M. On the composition of the passive film on Nickel: a surface-enhanced Raman spectroelectrochemical study[J]. J. Electroanal.. Chem., 1992, 333: 103.

[12] Maslar J E, Hurst W S, Bowers W J, et al. In-situ Raman spectroscopic investigation of aqueous iron corrosion at elevated temperatures and pressures[J]. J. Electrochem. Soc., 2000, 147: 2 532.

[13] Odziemkowski M, Flis J, Irish D E. Raman spectral and electrochemical studies of surface film formation on iron and its alloys with carbon in Na_2CO_3/ $NaHCO_3$ solution with reference to stress corrosion cracking[J]. Electrochim. Acta, 1994, 39: 2 225.

[14] Hugot-Le Goff A, Flis J, Boucherit N, Joiret S, Wilinski J. Use of Raman spectroscopy and rotating split ring disk electrode for identification of surface layers on Iron in 1M KOH[J]. J. Electrochem. Soc., 1990, 137: 2 684.

[15] Thierry D, Persson O, Leygraf C, Boucherit N, Hugot-Le Goff A. Raman spectroscopy and XPS investigation of anodic corrosion films formed on Fe-Mo alloys in alkaline solutions[J]. Corros. Sci., 1991, 32: 273.

实用电极材料体系的共焦显微拉曼光谱研究

杨 勇*, 储 炜, 南俊民, 陈旭光, 林祖赓

(厦门大学固体表面物理化学国家重点实验室, 化学系,
物理化学研究所, 福建 厦门 361005)

摘要: 本文简要介绍了实验室内有关利用共焦显微拉曼光谱于某些实用电极材料(表面)性能研究的结果. 具体的研究实例包括: 尖晶石锂锰氧化物中 Li^+ 的嵌入-脱出过程, AB_5-型金属氢化物电极表面氧化物的性能和钢筋电极表面钝化膜及其孔蚀过程.

关键词: Li^+ 的嵌入-脱出过程; 尖晶石锂锰氧化物; AB_5-型金属氢化物; 表面氧化物; 钢筋电极; 孔蚀过程; 共焦显微拉曼光谱